Anales Acad. Nac. de Cs. Ex., Fís. y Nat., tomo 58 (2017): 39-55.

METALS IN BIOLOGY: METALLOENZYMES AND THEIR BIOMIMETIC MODEL COMPOUNDS – PURPLE ACID PHOSPHATASE AND CATECHOL OXIDASE

Bernt Krebs

Institut für Anorganische und Analytische Chemie, Universität Münster, Corrensstrasse 36, 48149 Münster, Germany.
E-mail: krebs@uni-muenster.de

Abstract

Transition metals play an important role in biological processes as active sites in metalloproteins, especially in catalytically active metalloenzymes. Their functions reach from hydrolytic reactions to isomerizations, redox reactions, activation of dioxygen, nitrogen, methane, or carbon dioxide, to electron transfer processes, and to transport and storage functions. Multi-step biological elementary processes in the respiratory chains and in photosynthesis are impossible without the participation of metal ions. In the present paper, after a general survey some typical iron and copper proteins are presented, and their metal-directed hydrolytic and oxidative reactions are discussed. Purple acid phosphatases with dinuclear Fe-Fe and Fe-Zn active sites cleave biological phosphoric acid diesters with high efficiency. Catechol oxidases and tyrosinases with dinuclear Cu-Cu active sites oxidize phenols and polyphenols to quinones and melanines in important biological key reactions. The synthesis and functional investigation of bioinorganic model compounds for metalloenzymes can lead to interesting "bioanalogous" technical catalyst systems. Some examples of dinuclear iron and copper model complexes are reported.

Key words: Metalloenzymes, Iron and copper proteins, Model compounds, Purple acid phosphatases, Catechol oxidases.

Resumen

Metales en Biología: Metaloenzimas y sus Compuestos Modelo Biomiméticos – Fosfatasas Ácidas Púrpuras y Catecol Oxidasa. Los metales de transición desempeñan una importante función en los procesos biológicos como sitios activos en metaloproteínas, especialmente en metaloenzimas catalíticamente activas. Sus funciones abarcan reacciones hidrolíticas, isomerizaciones, procesos redox, activación de dioxígeno, nitrógeno, metano o dióxido de carbono, hasta transferencia de electrones y funciones de transporte y acumulación. Procesos biológicos elementales, en etapas múltiples, como los que ocurren en la cadena respiratoria y en la fotosíntesis son imposibles sin la participación de iones metálicos. En este trabajo, luego de una revisión general, se presentan ejemplos de algunas proteínas de hierro y cobre, discutiendo algunas de las reacciones hidrolíticas y oxidativas en las que participan. Las fosfatasas ácidas púrpuras, conteniendo sitios activos dinucleares Fe-Fe o Fe-Zn, producen la ruptura de diésteres biológicos del ácido fosfórico con elevada eficiencia. Las catecol oxidasas y tirosinasas con sitios activos dinucleares Cu-Cu, oxidan fenoles y polifenoles a quinonas y melaninas en reacciones de gran importancia biológica. La síntesis e investigación funcional de modelos bioinorgánicos para metaloenzimas puede conducir a interesantes sistemas "bio-análogos" útiles para la catálisis industrial. Se presentan algunos ejemplos de complejos-modelo dinucleares de hierro y cobre.

Palabras clave: Metaloenzimas, Proteínas de hierro y cobre, Compuestos modelo, Fosfatasas ácidas púrpura, Catecol oxidasas.

1. Introduction – Bioinorganic Chemistry and the Elements of Life

Among the chemical elements in all biological systems and life processes on our planet metal ions play a most important and essential role. There is virtually no biological reaction, from bacteria, fungi, and other micro-organisms, to plants, invertebrates, mammals and human beings which is not determined, in some stage of the complicated reaction paths, by an elementary process involving metal ions. It is well known that main group metals such as sodium, potassium, magnesium, or calcium are essential elements active in various functions such as signal transduction, electrolyte balance, bone and teeth formation, photosynthesis of plants and many others. [e.g. 1-5]

Even more variable and especially fascinating are the functions of the transition metal ions (mostly elements with only partially filled "open" d electron shells) which fulfill a wide variety of chemical functions in biology, in spite of their relatively low concentrations in the living systems. The most important of these transition elements are iron (Fe), copper (Cu), zinc (Zn), manganese (Mn), molybdenum (Mo), cobalt (Co) and nickel (Ni). Their typical reactivities reach from structural functions to the catalytic assembly and degradation of the organic compounds, to the transport and storage of electrons for a large variety of biological redox reactions, to the catalytic activation of small molecules such as O_2, N_2, CH_4, CO_2, and H_2 (normally rather unreactive at ambient conditions) to utilize them for biochemical processes, or to "organometallic" reactivity involving metal-carbon bonds such as in cobalamine. In Fig. 1 the main group and transition metals which are important for life processes are given in a periodic table representation. The figure also shows some transition metals important for medical and pharmaceutical applications. Table I shows, besides the essential nonmetals, a listing of the metals present in our human body, some of them in considerable quantities such as the dioxygen-binding iron in haemoglobin and myglobin and (surprisingly) zinc together with the trace elements from copper to molybdenum.

The key to the understanding of their structural chemistry and reactivity is their well-known tendency to form coordination compounds ("complexes") such as in the huge number of Werner-type coordination compounds in inorganic chemistry. This tendency to form coordination compounds with Werner-type bonding to ligands with typical oxygen, nitrogen, or sulphur functions leads to a dramatic scenery of "functional biological coordination chemistry". It turns out that the transition metal ions are mostly surrounded in the biological systems by three alternative types of chelating biological ligand systems: (1) the proteins (peptides) formed by the some 20 d-amino acids which offer (a) nitrogen (mostly in histidine), (b) oxygen (mostly carboxylates of aspartate or glutamate), and (c) sulphur functionalities (in cystein) as ideal chelating ligand atoms, (2) macrocyclic systems such as in porphyrins or corrins which offer most rigid and efficient chelate ligands, and (3) the nucleobases or phosphate groups of the nucleic acids which also offer ideal coordination capacities for harder (Mg, Ca) or softer metal centers, the latter bonded to the nitrogen functions of the nucleobases (preferentially to guanine). [e.g. 1-5]

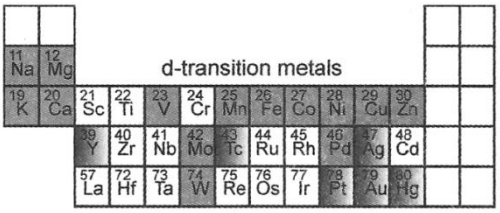

Fig. 1. Metals in life processes and in bioinorganic chemistry (shaded). In addition some metals (Y, Tc, Ag, Pt, Au, Hg) are indicated which are important for diagnostic and therapeutic applications in medicine

Table I. Elements of life: Nonmetals and essential metals in the human body (70 kg)

Element	Symbol	Mass (g)
Oxygen	O	45500
Carbon	C	12600
Hydrogen	H	7000
Nitrogen	N	2100
Calcium	Ca	1050
Phosphorus	P	700
Sulfur	S	175
Potassium	K	140
Chlorine	Cl	105
Sodium	Na	105
Magnesium	Mg	35
Iron	Fe	4 .2
Zinc	Zn	2 .3
Copper	Cu	0 .11
Manganese	Mn	0 .02
Selenium	Se	0 .02
Nickel	Ni	0 .01
Cobalt	Co	0 .003
Molybdenum	Mo	0 .003

The rather explosive development of research in the field of metals in biology during the last 30 years has led to the development of the active and exciting new discipline of Bioinorganic Chemistry (or Inorganic Biochemistry or Biological Inorganic Chemistry) at the borderline between the classical disciplines. As a typical "transdisciplinary" research field it resides between the established disciplines -besides inorganic chemistry and biochemistry- of biology, microbiology, toxicology, physiology, pharmacy, (bio)physical chemistry, and physics. The subjects of the field are the investigation of structures and functions of the metal sites in biological systems, including the study of catalysis in metalloenzymes, the dynamics and reaction paths and kinetics of the metal-assisted reactions, the bonding and transport and storage of metals in living systems, but also the toxicological aspects of metals in biology as well as the utilization of metals and metal compounds in medicine as diagnostic and therapeutic pharmaceutics. Well known examples for the latter are cis-platin and analogues as antitumor agents, gold anti-arthritic compounds or technetium complexes as radiopharmaceutical probes.

An important tool of bioinorganic chemistry research for the understanding of the *in vivo* structures and functions of metals is the *in vitro* synthesis and physical and functional investigation of biomimetic model complexes of metals which imitate the active sites of the metalloenzymes or other metalloproteins. They allow the study of structural and functional properties to be extrapolated to the biological systems to be modelled. Much of the successes of bioinorganic research can be attributed to the impressive development of physical methods such as EPR, NMR, MS, CV, X-ray diffraction, fast kinetic methods, or Mössbauer spectroscopy, which –in the light of often very low metal concentrations in the biological systems- have to be employed up to their limits if meaningful results are to be expected.

2. Transition Metals – Metalloproteins and Metalloenzymes

The field of metalloproteins as a central part of bioinorganic chemistry is at a growing stage of development. According to their electronic structure the most important d transition elements iron, copper, zinc, manganese, or cobalt, but also nickel, molybdenum, vanadium and others, use their specific chemical properties in the biological scene. Accordingly, iron, copper and manganese are essential as redox active centers in metalloproteins due to their ability to change redox states, i.e. to accept or release electrons. In contrast, zinc (also magnesium) are stable only in their oxidation numbers +2, making them ideal sites for acid/base reactions or for catalysis involving hydrolytic reactions. In Table II some typical functions of active metal sites in biomolecules are given.

Table II. Biological functions of selected transition metal ions in metalloproteins and metalloenzymes

Magnesium	structural function; hydrolases; isomerases
Cobalt	oxidases; alkyl transfer
Nickel	hydrogenases; hydrolases
Manganese	phostosynthesis; oxidases; structural function
Iron	oxidases; transport and storage of oxygen; electron transfer; nitrogen fixation
Copper	oxidases; transport of oxygen; electron transfer
Zinc	structural function; hydrolases

In the metal sites of the metalloproteins, one or multiple metal ions are bound to the protein by amino acid side chains and exogenous bridging and terminal ligands that define the first coordination sphere of each metal ion. These metal sites can be classified [6] into five types with the indicated functions:

(1) structural: configuration (in part) of protein tertiary and/or quaternary structure;
(2) storage: uptake, binding and release of metals in soluble form;
(3) electron transfer: uptake, release and storage of electrons;
(4) dioxygen binding: metal-O_2 coordination and decoordination;
(5) catalytic: substrate binding, activation, and turnover.

Coverage of the various metal sites has been summarized in several review articles. [5]

Here we present -as two typical examples for important types of enzymatically active metalloproteins- our work on two metalloproteins with dinuclear centers, purple acid phosphatase (an example of a dinuclear Fe-Zn protein) and catechol oxidase (an example of a dinuclear copper protein), and to relate the structure and the function, as far as it is possible today.

3. Iron as an Essential Bioelement and its Functions in Biology

The biochemistry of iron is essentially determined by its ability to change its oxidation states, generally from +2 to +3 and back, however especially during the reaction cycles of im-

portant metalloloenzymes, there exists also a fascinating chemistry involving higher oxidation states, especially Fe(IV). From haemoglobin and myoglobin to the variety of important iron-sulfur protein, its reactivity is determined by oxygen binding and transformation and redox reactions in addition to important electron transfer processes. Table III shows a short compilation of the essential iron-containing proteins in the human body. [1-6] In Fig. 2 a schematic overview is shown of the most important classes of iron proteins. As an example of one of them, the purple acid phosphatases with a dinuclear Fe-Fe or Fe-Zn site are highlighted in the figure. They are part of our research work, and they are addressed in some detail in the following.

Dinuclear Active Iron Sites - Purple Acid Phosphatases

Purple acid phosphatases (PAPs), E.C. 3.1.3.2, represent a group of ubiquitously distributed phosphomonoesterases. In Table IV some

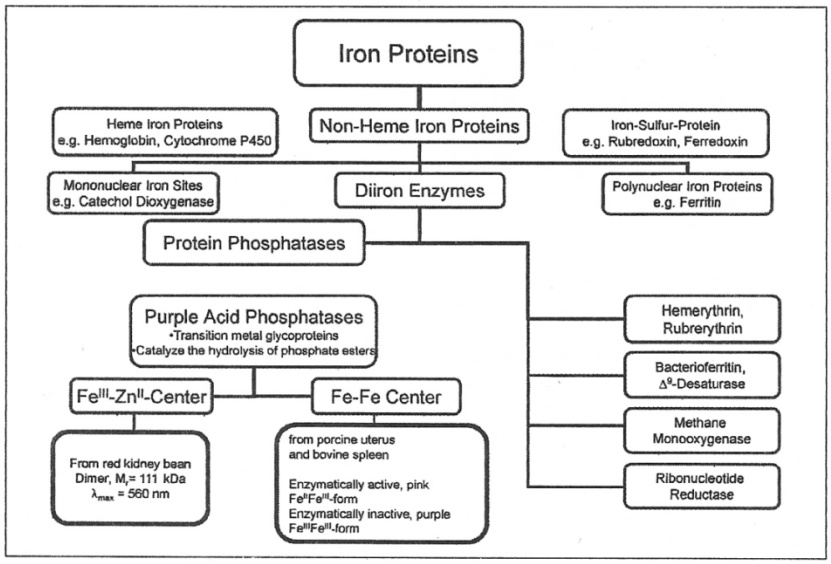

Fig. 2. Classification of iron proteins. Acid phosphatases are specially highlighted

Table III. Essential iron-containing proteins and enzymes in the human body

Protein	MW of the protein (kDA)	Amount of iron (g)	% of total iron in human body	Heme (h) or non-heme (nh)	Number of iron atoms per molecule	Function
Hemoglobin	64.5	2.60	65	h	4	oxygen transport in erythrocytes
Myoglobin	17.8	0.13	6	h	1	oxygen storage in muscles
Transferrin	76	0.007	0.2	nh	5	iron transport in blood plasma
Ferritin	444	0.52	13	nh	up to 5000	iron storage in cells
Hemosiderin	≥300	0.48	12	nh	up to 5000	iron storage in cells
Catalase	260	0.004	0.1	h	4	oxidation with hydrogen peroxide
Peroxidases	var.	low	low	h	usually 1	oxidation with hydrogen peroxide
Cytochrom c	12.5	0.004	0.1	h	1	electron transfer
Cytochrom c oxidase	≥100	0.02	0.5	h	2	terminal oxidation to water
Flavoprotein oxygenases (e.g. P-450)	ca. 50	low	low	h	1	insertion of molecular oxygen
Iron-sulfur proteins	var.	0.04	1	nh	2 – 8	electron transfer
Ribonucleotide reductase	260 (E. coli)	low	low	nh	4	transformation of RNA to DNA

typical mammalian and plant purple acid phosphatases are reported. They are all characterized by low pH-optima and intense color, which results from a tyrosine → Fe(III) *charge transfer* transition. [7] The intense *charge transfer* band ($\varepsilon \geq 3000\ M^{-1}\ cm^{-1}$ per iron) can be used as a probe for electron density of the ferric ion. In mammalian PAPs a second iron occupies the "nonchromophoric site", which is divalent in the active state and trivalent in inactive state. Monomeric 35 kDa mammalian PAPs exhibits a shift from 550 to 510 nm upon reduction from purple inactive Fe(III)-Fe(III) to the pink active Fe(III)-Fe(II) form. [8] The nature of the metal in the nonchromophoric site varies in plant PAPs. It is zinc in kidney bean PAP (kbPAP), in soybean PAP and in one of the three known sweet potato isoenzymes (spPAP), whereas in another spPAP isoenzyme the nonchromophoric site is occupied by whose oxidation state is not yet known. [9-11]

The dinuclear metal center has attracted considerable interest and is now spectroscopically well characterized by Mössbauer, [12,13] EPR, [8, 12, 14-17] NMR, [16, 18, 19] EXAFS, [20-22] magnetic, [12, 23-25] electrochemical, [26] and Resonance Raman [27, 28] studies.

The mixed-valent diiron form of mammalian PAPs shows rhombic EPR spectra with $g_{ave} \sim 1.74$, characteristic for an antiferromagnetically coupled high spin Fe(III)-Fe(II) pair, arising from a S = 1/2 ground state. The oxidized diferric form of PAPs are EPR silent due to antiferromagnetic coupling of two high spin Fe(III) ions with S = 0. Native kbPAP has no signal around g = 1.7, but shows a signal at g = 4.3, characteristic for isolated high spin Fe(III) with S = 5/2 ground state as expected for the Fe(III)-Zn(II) active site. After exchange of zinc by iron, the EPR spectrum of the diiron substituted kbPAP resembles that of mammalian enzymes, just as the iron-zinc substituted mammalian PAPs show similar EPR spectra as native kbPAP. The magnetic coupling constant -J of the mixed-valent state of bovine spleen PAP (bsPAP), porcine uterus PAP (uteroferrin, Uf) and zinc-exchanged diiron kbPAP was typically found to be 6-20 cm^{-1}, which is consistent with the presence of a μ-hydroxo rather than a μ-oxo as the bridging ligand. The diiron centers of bsPAP and Uf and the Fe-Zn centers of kbPAP, spPAP and Uf have been subjected to XAS measurements. XAS spectra reveal a N/O donor set. A short Fe-O bond, which is characteristic of a μ-oxo bridge, was not found, in agreement with the magnetic measurements described above. Metal-metal distances of 3.0-3.3 Å for mammalian PAPs are in good agreement with the ones determined by X-ray structural analysis. A longer iron-zinc distance of 3.9 Å has been determined for kbPAP by EXAFS analysis.

The first PAP crystals were reported for the kidney bean enzyme grown from ammonium sulfate in tetragonal space group $P4_32_12$. [29] Some years later Sträter *et al.* succeeded in obtaining kbPAP crystals in orthorhombic space group $C222_1$ which enabled successful structure determination with a resolution of 2.9 Å. [30]

The crystal structure of a plant acid phosphatase: kidney bean phosphatase (kbPAP)

Overall structure and folding. The structure of the homodimeric kbPAP [30, 31] has the shape of a lung with overall dimensions 40 x 60 x 75 Å. Each monomer of kbPAP consists of

Table IV. Purple acid phosphatases

Source	MW (kDa)	Subunits	Metal content	pH optimum
mammalian sources				
human spleen	34	1	2 Fe	5.5
human macrophage	36	1	2 Fe	5.6
bovine spleen	35	1	2 Fe	5.8
rat spleen	33	1	2 Fe	5.7
bovine bone	32	1	?	5.5
rat bone	41	1	2 Fe	?
porcine uterus	36	1	2 Fe	5.0
plant sources				
kidney bean	111	2	1 Zn, 1 Fe	5.8
sweet potato	113	3	1 Fe, 1 Zn/Mn	5.8
soy bean	240	4	2 Mn	?
spinach	92	2	?	5.5
rice	94	2	2 Mn	5.5

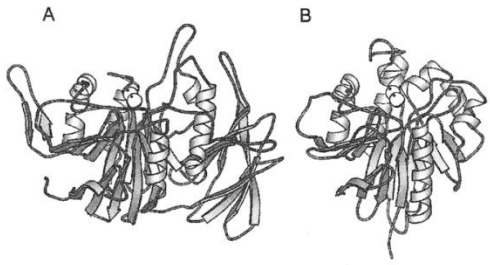

Fig. 3. Molecular structures of (A) kidney bean purple acid phosphatase (plant, kbPAP) and (B) of the mammalian phosphatase uteroferrin from X-ray crystal structure analysis

two subunits (Fig. 3 A). The smaller N-terminal domain consists of 120 amino acid residues containing only β-strands. The C-terminal α/β-domain exhibits two β-α-β-α-β motifs harboring all residues involved in metal binding. This motif is also found in other phosphoester hydrolyzing enzymes with a dinuclear center like protein phosphatase 1, calcineurin [32-34] and a 5'-nucleotidase. [35]

The dinuclear Fe(III)-Zn(II) site. The active site is located on the edge of the β-sandwich core structure, easily accessible to the solvent and presented in Fig. 4. The Fe(III) is coordinated by Tyr157, which is obviously responsible for the *charge transfer* band and the color, by N_ε of His325 and monodentately by the carboxylate group of Asp135. The zinc ion in the nonchromophoric site is coordinated by N_ε of His286, N_δ of His323 and the amide oxygen of Asn201. Both metal ions are bridged monodentately by the carboxylate group of Asp164 and by a hydroxide. For both metal ions the octahedral coordination sphere is thought to be completed by two exogenous water-derived ligands in the native protein, hydroxide at the chromophoric iron and water at the nonchromophoric zinc. This ligands could unfortunately not resolved in the X-ray structure but were modeled in the coordination sphere based on spectroscopic and kinetic data. [8, 36] The distance between the two metals was refined to 3.2 Å. [30, 31]

Crystal structure of inhibitor complexes. The comparison of X-ray structures of the inhibitor complexes with phosphate and tungstate revealed the same bridging binding mode for both inhibitors replacing exogenous water-derived ligands. [31] No larger conformational changes in enzyme structure occurred when oxoanion bind the active site. Small shifts

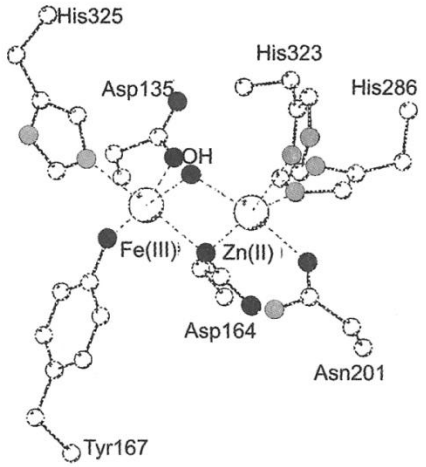

Fig. 4. The heterodinuclear active site in purple acid phosphatase from kidney bean (kbPAP)

up to 1 Å were observed for active site residues His295 and His296. Inhibitors are furthermore located in hydrogen bonding distance to His202. Bidentate bridging of phosphate is also seen in X-ray structures of mammalian PAPs. [37-39]

Comparison of mammalian and plant PAP structure

Overall structure and folding. Despite low sequence homology, different subunit arrangements (monomeric vs. homodimeric) and different metal content, mammalian and plant PAPs have an almost identical fold of the active site domain, predicted by comparative modeling [40] and now confirmed by crystal structures of rat and pig PAP (Fig. 3 A + B). Superposition of rat and kidney bean structures resulted in 214 equivalent α-carbon atoms with a root mean square deviation (rmsd) of 1.43 Å. Apart from obvious differences in N-terminal domain some minor changes in secondary structure can be recognized. The most striking difference with impact on activity of mammalian enzymes is the loop between α5 and α6, which is missing in the plant enzyme, and renders the active site of the intact enzyme less accessible for the substrate. This loop, also called repression loop, [39] is easily cleaved by serine and cysteine proteases [41] with the subunits formed tethered together by disulfide bridge between Cys142 and Cys200. This cleavage leads to a 3- to 9-fold activation of enzyme activity with para-nitrophenylphosphate as substrate.

Comparison of metal coordinating region. X-ray structures of mammalian and plant PAPs showed nearly identical first coordination spheres, [37] but differences in the second sphere exists. In the kbPAP structure His202, His295 and His296 come into hydrogen-bonding distance to the coordinated phosphate group and are supposed to play an essential role in stabilizing the transition state by electrostatic interaction and in protonating the leaving group. [31] Two of these histidine residues (His202 and His296) have their structural counterparts in His92 and His195 in mammalian PAP structures, but His295 of kbPAP is replaced by Glu194 in mammalian PAPs which points away from the active site and is not in close contact to the phosphate group.

Reaction mechanism. In a plausible mechanism [8, 31, 36] (Fig. 5) the phosphate group of the substrate binds to the divalent metal ion, which together with the histidine ligands preorients the phosphate group and enhances the electrophilicity of the phosphorous center. Then a nucleophilic attack occurs by the hydroxide ligand bound to the Fe(III) center, and the configuration at the phosphorous center is inverted through a pentacoordinate transition state with the leaving group and the attacking nucleophile in apical positions. In Fig. 6 this proposed transition state is shown in a modeled representation. In addition to the metal ions the protonated side chains of His202 and His296 reduce the energy of the pentacovalent transition state through the formation of hydrogen bonds. After a small movement, His295 may also interact with the substrate and His296 may then protonate the leaving alcohol group.

Another suggestion for a reaction mechanism considers the terminal bound hydroxide activates as base another water molecule from the second coordination sphere of the ferric ion which than acts as the nucleophile. [42, 43] Others expect the bridging hydroxide to act as a nucleophile. [44]

Physiological Role

Function of PAP in plants. Due to high in vitro activity of the kidney bean enzyme for ATP, a role as ATPase was suggested. [9] Based on immunochemical techniques this protein was localized in ribosome-rich areas in cells from seeds of dry red kidney beans and a role in triggering seed dormancy was proposed. [45] The

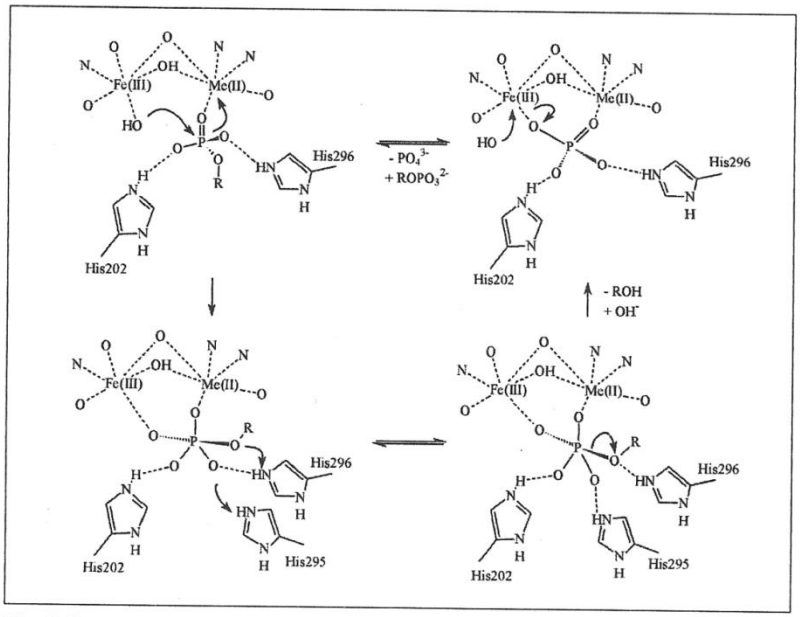

Fig. 5. Proposed reaction mechanism for phosphoric ester hydrolysis catalyzed by purple acid phosphatases. Me(II) can be iron (such as in mammalian PAPs), manganese, or zinc (in kidney bean phosphatase)

enzyme isolated from thale cress (atPAP) resembles in primary structure more mammalian than plant enzymes and exhibits phosphatase and peroxidation activity. [46] The authors concluded that atPAP could be involved in phosphate mobilization and in metabolism of reactive oxygen species in stressed or senescent plant organs.

Function of mammalian PAPs. Whereas plant PAPs are often described as hydrolyzing enzymes, different modes of action are described for mammalian PAPs. In pig and horse, PAPs are found to be secreted in the uterus of pregnant animals under control of progesterone. [5, 37] The hypothesis was advanced that PAP in this organ is responsible for porcine transplacental iron transport. [39, 40] Localization studies linked PAP to osteoclasts and elevated levels of this enzyme were found to be associated with pathological enhanced bone. [46, 47] Several modes of action have been described for PAP in bone metabolism and the reader is addressed to the literature. [47-50] In 1987 it was reported that PAP plays a role in degrading phagocytized erythrocytes, based on its localization in lysosomes and lysosome-like organelles of these macrophages. [51] A recent study demonstrated that PAP expression was not restricted to spleen and bone, but was also detectable in liver, lung, heart, kidney, stomach, small intestine and skin. [52] A new chapter has been opened very recently by the successful structure determination of two human purple acid phosphatases. [53]. Other recent developments include porcine PAP [57] besides new work on plant PAPs. [54-56]

Biomimetic Model Complexes for Purple Acid Phosphatases

Since the detection of the purple acid phosphatases and the probable nature of their active sites a considerable number of synthetic and physicochemical studies have been reported on the structural and functional properties of biomimetic model compounds. Besides various models with Fe-Fe sites a special preparative challenge was the synthesis of heterodinuclear models for the Fe-Zn site in purple acid phosphatase from plants, especially from kidney beans. Some examples were synthesized and investigated recently in our laboratory, partly in cooperation with partners. [58-60] Two examples are shown in Fig. 7. It has been stressed that an essential part of the investigations is the identification of physical properties relevant to the biological functions of metalloenzymes. In Fig. 8 an example is given for such physicochemical investigations on enzymes active sites and on model complexes. It shows the determination of redox potentials of iron-containing centers indicating the potentials to reduce Fe(III) or to oxidase Fe(II). The Fe-Fe center shows two redox steps whereas the Fe-Zn site shows only one step because of the stability of Zn(II) towards oxidation.

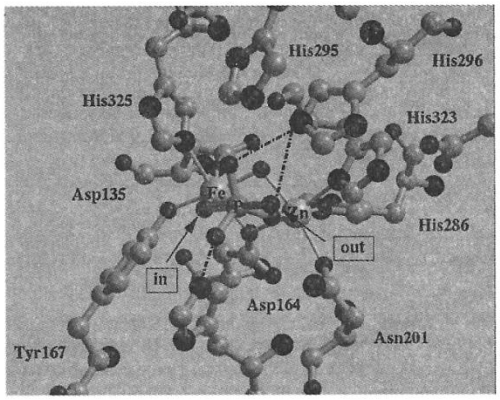

Fig. 6. Model of the transition state with pentacoordinate phosphorus in the catalytic reaction of purple acid phosphatase from kidney beans

4. Copper Proteins and Functions of Copper Enzymes

Besides iron and zinc, copper is the most ubiquitous transition metal in life processes. In Table V some typical important copper proteins for catalysis and metal transport/storage are listed.

Copper Type 3 Proteins – Their Dinuclear Active Sites

The copper enzymes tyrosinase, catechol oxidase as well as the oxygen transport hemocyanin comprise the type 3 class within the large number of different copper protein. Some of their important properties and their dioxygen binding mode are shown in Fig. 9.

Catechol Oxidase

Catechol oxidases (CO), E.C. 1.10.3.1, represent a group of ubiquitous oxidases in plants. CO, tyrosinase (TYR), E.C. 1.14.18.1 and E.C. 1.10.3.1, and hemocyanin (HC) belong to the class of copper type 3 centers characterized by an antiferromagnetically coupled ($-2J > 600$ cm^{-1}) EPR silent Cu(II) pair in the *met* form, i.e. the oxidized form with no dioxygen bound to the metal center, and two intense absorption maxima at 350 nm (ε 19,000 cm^{-1} M^{-1}) and 600

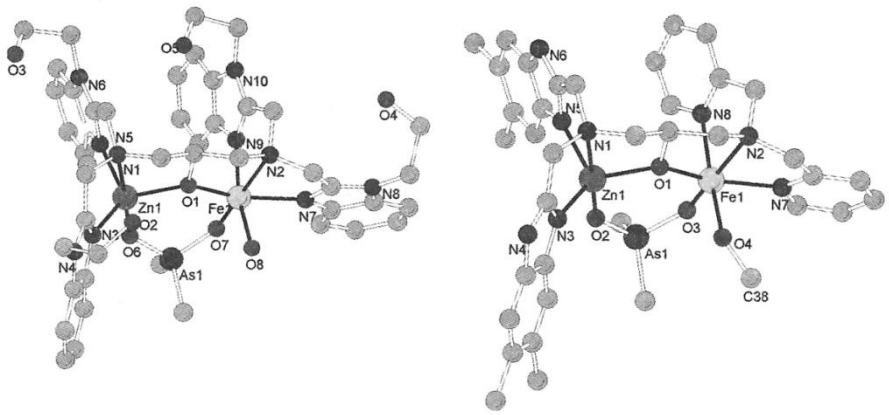

Fig. 7. Biomimetic model complexes for the active site of purple acid phosphatase with hetero-dinuclear Fe-Zn sites

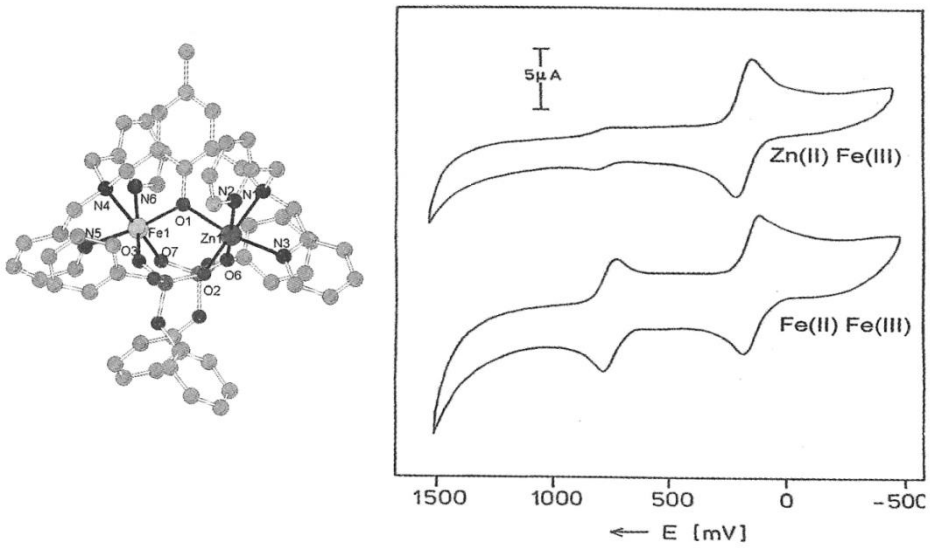

Fig. 8. Measurement of redox potentials by cyclic voltammetry (CV) of Fe-Zn and Fe-Fe model complexes for purple acid phosphatases

nm (ε 1,000 cm^{-1} M^{-1}) caused by $O_2^{2-} \rightarrow$ Cu(II) *charge transfer* transitions in the *oxy* form.

CO catalyzes exclusively the oxidation of catechols (i.e. *ortho*-diphenols) to the corresponding *ortho*-quinones (catecholase activity). In contrast to CO the related TYR reveals in addition to catecholase activity a monooxygenase activity (cresolase activity, E.C. 1.14.18.1) that enables the enzyme to accept monophenols, e.g. tyrosine, as substrate. HC is the oxygen transport protein in many molluscs and arthropods. The dicopper center is spectroscopically well characterized by UV/Vis, EPR, NMR, EXAFS, magnetic and Resonance Raman studies. [61]

The *met* form of CO contains two Cu(II) ions but exhibits no EPR signal due to strong antiferromagnetic coupling between the two S = 1/2 metal ions. The antiferromagnetic coupling requires a superexchange pathway associated with a bridging ligand which is most likely a μ-hydroxo group bridging the two Cu ions. *Oxy* CO can be obtained by adding H_2O_2 to *met* CO. Evidence for the oxygen binding mode can be derived from UV/Vis data in combination with Reso-

Table V. Selected copper proteins and their functions

Protein	Reactivity	Biological function and occurrence
Type 1 copper proteins		
Plastocyanin		Electron transfer in plants (Fig.)
Azurin		Electron transfer in bacteria
Type 2 copper proteins		
Amine Oxidase	Oxidase	Metabolism of amines in bacteria, yeast, plants, mammals (Fig.)
Dopamine ß-monooxygenase	Dioxygenase	Oxidation of dopamine in kidney (Fig.)
Quercetin Dioxygenase	Dioxygenase	Cleavage of quercetin in fungi (Fig.)
Galactose Oxidase	Oxidase	Oxidation of alcohols in fungi (Fig.)
Cu, Zn Superoxide dismutase	Dismutase	Disproportionation of superoxide, e.g. in erythrocytes
Type 3 copper proteins		
Hemocyanin		Dioxygen transport in molluscs and arthropods
Tyrosinase	Oxygenase and Oxidase	Hydroxylation of phenols (Fig.) *o*-Quinone formation in mammals and plants
Catechol Oxidase	Oxidase	Oxidation of catechols to *o*-quinones (plants)
Non-classical copper proteins		
Copper Transport ATPase	Thionein	Regulation, strorage, and transport of Cu
Cytochrome c Oxidase		Electron transfer in respiratory chain (Cu_A)
N_2O Reductase	Reductase (Cu_A)	Reduction of N_2O to N_2 in nitrogen cycle
Laccase	Oxidase (type 2+3)	Oxidation of polyphenols and –amines in plants
Ascorbate Oxidase	Oxidase (type 2+3)	Oxid. of ascorbate to deydroascorbate in plants

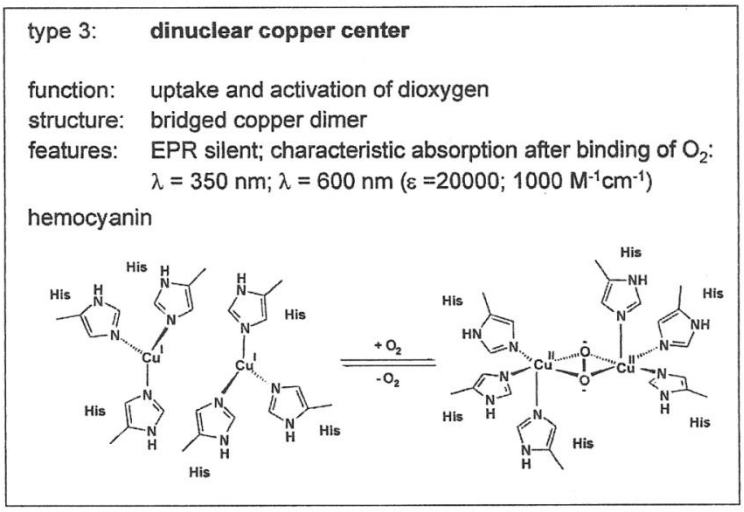

Fig. 9. Copper in metalloproteins: type 3 dinuclear active sites in catechol oxidase, tyrosinase, and hemocyanin

nance Raman data of the *oxy* form. *Oxy* CO shows two characteristic peroxo → Cu(II) charge transfer transitions. The absorption band at 345 nm is caused by an O_2^{2-} (π^*_σ) → Cu(II) ($d_{x^2-y^2}$) *charge transfer* transition. The absorption band at 580 nm corresponds to the second O_2^{2-} (π^*_v) → Cu(II) ($d_{x^2-y^2}$) *charge transfer* transition. The Resonance Raman spectrum of the *oxy* form shows a band ~ 750 cm^{-1} characteristic for a μ-η^2:η^2 bonding mode for dioxygen first reported by Kitajima et al. [62]

for a synthetic binuclear copper model complex. EXAFS studies of *Neurospora crassa* TYR and sweet potato CO revealed a Cu(II)-Cu(II) distance of 3.6 Å and 3.8 Å, respectively for the *oxy* species and 3.4 Å and 2.9 Å, respectively for the *met* form. [63] The first shell is reported to consist of two nitrogen and oxygen ligands in the *met* form.

For several years, two arthropodan HC crystal structures were available, spiny lobster (*Panulirus interruptus*) [64] and horseshoe crab (*Limulus polyphemus*).[65] Recently, a molluscan HC could be crystallized and its three-dimensional structure determined [66] from giant octopus (*Octopus defleini*). Up to now a protein structure of TYR is not available. In 1998 we succeeded in obtaining CO crystals from sweet potato (*Ipomoea batatas*, ibCO) grown from PEG 6000 at pH 7.0 with 500 mM NaCl in monoclinic ($P2_1$) and orthorhombic space group ($P2_12_12$) for successful structure determination of the first type 3 copper enzyme. [67]

The crystal structure of a plant CO containing a dinuclear copper center

Overall structure and folding of ibCO. Monomeric ibCO, with a molecular mass of 39 kDa, is ellipsoid in shape with dimensions of 55 x 45 x 45 Å (Fig. 10). The secondary structure is dominated by α-helical and coiled regions. The structure shows a four helix bundle surrounding the dinuclear copper center as the most striking structural motif. Two disulfide bridges (Cys11 to Cys28 and Cys27 to Cys89) help to anchor the N-terminal region of the protein (residues 1 to 50) to the core of the enzyme.

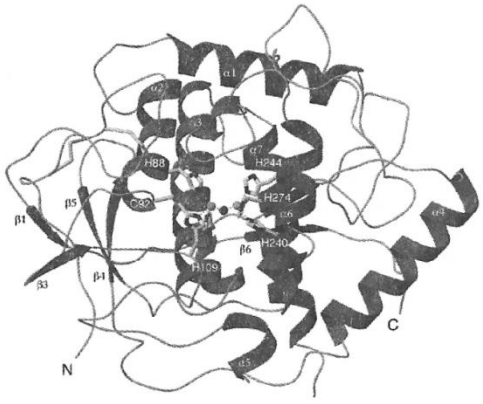

Fig. 10. Structure of catechol oxidase from sweet potato (*Ipomoea batatas*) determined by X-ray diffraction

The dinuclear copper site including a covalent cysteine-histidine bond. Both of the two copper atoms are coordinated by three histidine residues contributed from the four helices of the α-bundle (Figs. 10 and 11). Both CuA and CuB are coordinated by N_ε of histidine residues (His88, His109, His118 to CuA, and His240, His244, His274 to CuB). An interesting feature of the dinuclear metal center in ibCO is a covalent thioether bond formed between C_ε of CuA-coordinating His109, and S of Cys92. There are also reports for cysteinyl-histidyl units for TYR from *Neurospora crassa* [68] as well as for HC from *Helix pomatia*. [69] The recently published structure of the functional subunit of HC from *Octopus dofleini* reveals that one of the six histidine ligands is also involved in a thioether bridge. [66] The absence of the cysteinyl-histidyl bridge in HCs from arthropods and human TYR, however, does not support its direct involvement in the electron transfer process. The structural motif of a thioether bond has also been described for the mononuclear copper enzyme galactose oxidase. Here, the covalent bond is formed between the C_ε carbon of a tyrosinate ligand and the sulphur of a cysteine and stabilize the tyrosine radical generated during catalysis. [70] The involvement of the Cys-His bridge in the catalytic pathway of CO is therefore possible, but a structural function is not less probable.

In the oxidized *met* CO structure solved at a resolution of 2.5 Å the two cupric ions are 2.9 Å apart. [67] Most likely they are bridged by a hydroxide ion completing the four-coordinate trigonal pyramidal coordination sphere. EPR data reflect an antiferromagnetically coupled EPR silent Cu(II)-Cu(II) state [63, 71] of the enzyme which is in good agreement with a μ-hydroxo group bridging the copper atoms observed in the crystal structure.

Crystal structures of the reduced form and the phenylthiourea inhibitor complexes

Reduced form: The crystal structure of the reduced form exhibits a resolution of 2.7 Å. Upon reduction of the enzyme to the Cu(I)-Cu(I) state the metal-metal separation extends significantly to 4.4 Å, whereas the histidines move very little. No significant conformational change is observed for the rest of the protein. A water molecule was positioned coordinated to CuA. In the reduced state the coordination sphere of CuA thus matches a distorted tetrahedron, whereas the coordination of CuB can be described as square planar with one missing coordination site.

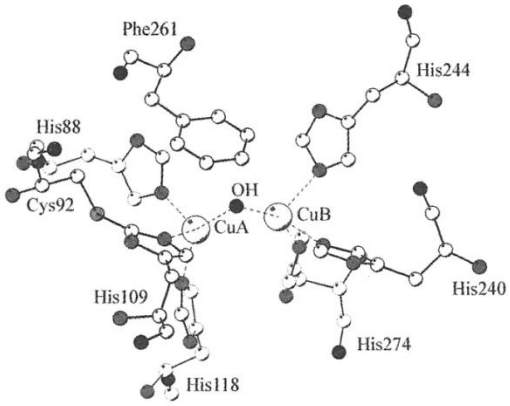

Fig. 11. Structure of the active site of catechol oxidase from *Ipomoea batatas*

The coordinating residues are moving less indicating a rather rigid pocket. The coppers atoms are moving primarily leading to a changed coordination sphere.

Inhibitor complex: A crystal structure with a substrate analogue inhibitor was solved at a resolution of 2.7 Å. The inhibitor complex revealed conformational changes of the residues in the active site which indicated that access to the catalytic metal center is primarily controlled by rotation of the aromatic ring of Phe261 (see also Fig. 11). Upon binding of phenylthiourea (PTU) the phenyl ring of Phe261 and the imidazole ring of His244 undergo a conformational change to form hydrophobic interaction with the aromatic ring of the inhibitor. The sulphur of phenylthiourea replaces the hydroxo-bridge, present in the Cu(II)-Cu(II) enzyme, and coordinates both copper ions, thereby increasing the metal-metal separation to 4.2 Å. The amide nitrogen interacts weakly with CuB (Cu-N 2.6 Å) completing its square-pyramidal coordination sphere. In addition to the interaction with the dicopper center van der Waals interaction of the residues line the hydrophobic cavity (Phe261, Ile241, His244) contributing to the high affinity of the PTU to the enzyme.

Comparison of the CO structure with the different HC structures. HCs can be divided into arthropodan (e.g. from lobsters and spiders) and molluscan (e.g. from octopus and snails) isozymes. Since arthropodan and molluscan HCs differ in sequence and tertiary structure and subunit organisation comparison of the ibCO crystal structure is performed with both classes, respectively.

Overall structure and folding. Comparison of the ibCO structure with the two arthropodan HC (*Panulirus interruptus* [64]and *Limulus polyphemus* [65]) structures revealed the existence of an additional N-terminal region for HC located above the dinuclear copper center. This region seems to hinder free access of possible substrates to the copper center of HC and thus may function as a shield above the metal center.

Comparison of ibCO structure and the only available and molluscan HC structure from *Octopus dofleini*, subunit g, (odgHC) [66en ibCO and odgHC sequence is rather low (about 25%) but the structural similarity is remarkably high with a root mean square deviation of 1.27 Å for 701 backbone atoms, [72] which seems surprising taking into account the evolutionary distance between molluscan and higher plants. The tertiary folding of ibCO and molluscan HC is nearly identical including the regions apart from the four helix bundle motif. Again, the HC protein is larger in mass. Here, an additional C-terminal region of molluscan HC is positioned as a shield above the metal center.

Comparison of metal coordinating region. As in the case of ibCO the dicopper center in the arthropodan HC structures from *Panulirus interruptus* and *Limulus polyphemus* is buried between the α-helices of a four helix bundle. All six histidine residues coordinating the Cu are provided by these α-helices. [73] Additionally, the Phe residue of this shielding region reaches into the pocket of the oxygen binding site of arthropodan HC. This phenyl ring aligns perfectly with the aromatic ring of phenylthiourea in the inhibitor complex of ibCO. This residue prohibits any binding of substrate and consequently permits HC to function only as an oxygen storage and transport protein. Interestingly, this fully conserved Phe residue is proposed to be the key residue in the allosteric regulation mechanism postulated for HCs.

Comparison of the catalytic cores of ibCO and odgHC reveals similar results [72] except the mutation of the Phe residue to Leu residue in *Octopus dofleini* crystal structure. This is interesting as HC from *Octopus vulgaris* is reported to exhibit a weak catecholase activity. [74] The Leu residue may be less effective in hindering substrate binding and therefore be responsible for this additional activity. But since sequence and structure of the *Octopus vulgaris* isozyme are not reported yet, there is no prove that Leu is present in the active site of this isozyme, too.

Reaction mechanism. The proposed catalytical pathway (see Fig. 12) is a combination

of biochemical, spectroscopic and structural data. In ibCO the rotation of the side chain of Phe261 opens the catalytic pocket of the copper center (not shown in Fig. 12) as it is positioned in the way the substrate must pass to reach the copper center (see Fig. 11). It therefore might influence substrate specificity of the enzyme by suppressing accession of sterically pretentious substrates. Inside the pocket a glutamate residue Glu251 and an isoleucine residue Ile243 are positioned. The glutamate residue is supposed to be involved in dehydrogenating the substrate whereas the isoleucine residue seems to be involved in tuning the substrate specificity.

Based on the binding mode observed for the phenylthiourea complex of CO a monodentate binding mode of the substrate is favored, in which the catechol substrate binds after deprotonation of one of the two hydroxyl groups to CuB. The first substrate molecule binds to the *met* form, which is the state present after purification. Once the quinone is formed the Cu center remains in its reduced state with one copper containing a water solvent molecule (Fig. 12). Now oxygen binds to the reduced form. UV/Vis spectroscopic results in combination with Resonance Raman investigations suggests that molecular oxygen binds as peroxide in a μ-η^2:η^2 binding mode with a metal metal separation of 3.8 Å as determined by EXAFS spectroscopy. [63] The same binding mode for dioxygen has been determined for the oxygenated *Limulus polyphemus* HC with a Cu-Cu separation of 3.6 Å. Binding of the second substrate molecule leads to a CO-O_2^{2-} substrate complex modeled with the aid of PTU*CO inhibitor complex. [67] In this model, CuB would be six-coordinated with a tetragonal planar coordination by His240, His244 and the dioxygen molecule. The two axial positions would be occupied by His274 and the catechol substrate. The CuA site would possess a tetragonal-pyramidal coordination with His88, His118 and O_2^{2-} in equatorial His109 in an axial position and a vacant non-solvent accessible sixth coordination site. In this proposed CO-O_2^{2-}-substrate complex, two electrons could be transferred from the second substrate molecule to the peroxide, followed by cleavage of the O-O bond, loss of water and departure of the o-quinone product. The catalytic mechanism of TYR was studied by Solomon et al., [75, 76] which also includes a mechanism for catecholase activity, the second activity TYR exhibits. In TYR catecholase activity can start both from the *oxy* and *met* form, as both are present in the resting form of TYR. The mechanism is very similar to the one of CO, described above. Alternative reaction mechanisms for TYR differing slightly have also been proposed. Additionally,

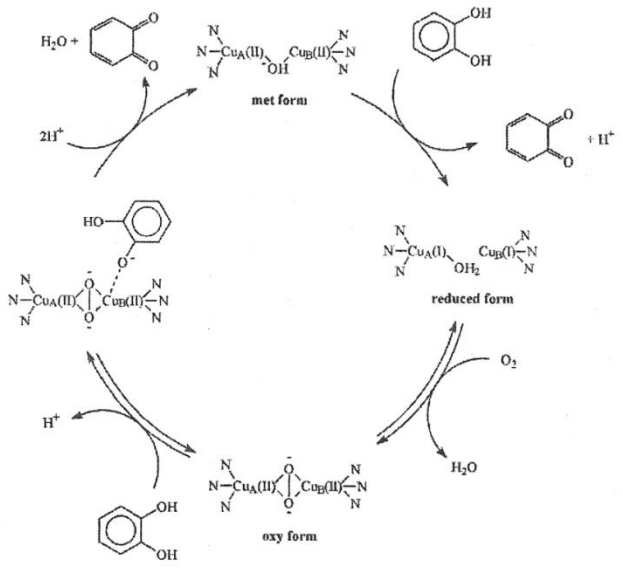

Fig. 12. Proposed reaction pathway of catechol oxidase

a radical mechanism has been favoured by Kitajima et al. [77] and a Cu(III) intermediate based on model compound investigations was suggested. [78, 79] These suggestions might also be important for the mechanism of CO, but with the absence of a crystal structure of TYR it is difficult to enlighten distinct mechanistic differences of CO and TYR.

Physiological Role. There were several proposed functions for CO in higher plants, but none of them could really be established. The most evident proposed possible function of plant CO is a role in disease defense of higher plants. [80] The enzyme is cytosolic or membrane-bound whereas possible substrates are kept separated in the vacuole. After disruption of the cell by wounding or infection the membrane is lysed and these two components can come in contact forming quinones to polymerize to melanins. CO mRNA has been found to be upregulated after wounding or infecting in apples. [81] Furthermore, some parasites have been found to use inhibitors of the CO indicating the CO/diphenol system a hurdle to take for colonization of the parasite's host. Other proposed physiological roles are pigment formation and oxygen scavenging in the chloroplast. [80, 82] Recently, the function of pigment formation in flowers was related to auresidin synthase, a catechol oxidase homologue. [83]

In mammals TYR starts forming skin pigmentation. [80] The absence or inactivation of the enzyme leads therefore to forms of albinism (tyrosinase-negative albinism and ocultaneous albinism). In insects TYRs are involved both in sclerotization and defense.

Biomimetic Model Complexes for Catechol Oxidase and Tyrosinase

Dinuclear peroxo copper(II) compounds. A wide range of work has been done in the field of biomimetic model compounds for type 3 copper proteins that has been summarized in a number of articles. [84-93] Model compounds of the active site of copper type-3 proteins played an important role in elucidating the binding mode of dioxygen in the oxy form. A rather comprehensive discussion of these compounds was recently given in *J. Argent. Chem. Soc.* [94] so that only a few details are repeated here.

In 1988 the first crystal structure for a peroxo copper(II) complex using the ligand tris[(2-pyridyl)methyl]amine (tpa) was reported. In a self assembly reaction of the monomeric Cu(I)(tpa) precursors with molecular oxygen the thermally unstable complex $[(Cu(tpa))_2(O_2)]^{2+}$ was obtained at low temperatures. The peroxo group is bound in a *trans* μ-1,2 bridging mode. [95] This complex represents the first functional model for oxy hemocyanin, the spectroscopic and structural qualities, however, do not fit to those of the protein. In 1989 Kitajima [96] succeeded with the first synthesis of a side on μ-η^2:η^2 peroxo copper(II) complex employing the ligand hydrotris(3,5-diisopropyl-1-pyrazolyl)borate (HB(3,5-iPr2pz)3) (see Fig. 13). Preparation of the complex was performed at low temperatures either by the reaction of a monomeric Cu(I) complex with O_2 or by adding excess of H_2O_2 to dinuclear μ-oxo or di-μ-hydroxo bridged copper(II) complexes. This model compound exhibits similar magnetic, spectroscopic and structural features compared to the *oxy* form of HC. In 2001 the crystal structure of another side on μ-η^2:η^2 peroxo copper(II) complex with the modified ligand hydrotris(3-trisfluoro-5-methyl-1-pyrazolyl)borate was reported. [97] The first room temperature stable side on μ-η^2:η^2 peroxo copper(II) complex was reported in 1999. It contains a dinucleating ligand that provides three aromatic nitrogen donor atoms for each copper atom. [98]

Cresolase activity of copper complexes. With the complex $[Cu_2(L\text{-}66)]^{2+}$ (with L-66 = α,α'-bis[bis[2-(1'-methyl-2'-benzimidazolyl)ethyl]amino]-m-xylene the first model compound was presented that was able to bind dioxygen reversibly followed by oxidation of a phenol to the corresponding catechol. [99] This biomimetic model complex represents the first operating tyrosinase model system, that imitates the cresolase activity of metalloenzymes Synthetic efforts to prepare model complexes for the binding of the phenolic oxygen in the course of the catalytic cycle of tyrosinase resulted in a first complex based on the asymmetric ligand N-(2-hydroxybenzyl)-N,N',N'-tris[(2-pyridyl)methyl]-1,3-diaminopropan-2-ol (Hbtppnol) containing a

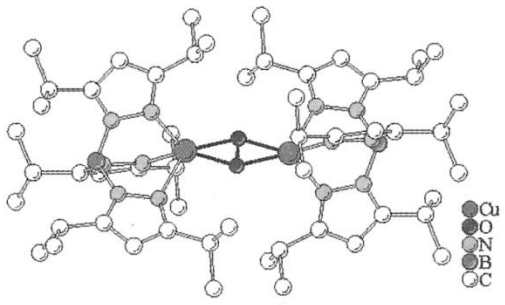

Fig. 13. The first biomimetic copper complex with dioxygen bonding as a model for type 3 copper proteins

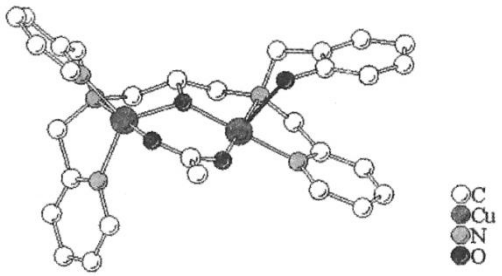

Fig. 14. Biomimetic model complex for type 3 copper proteins with a non-deprotonated phenol group

non deprotonated phenol group on one of the two copper atoms (see Fig. 14). [100-102] This complex can be regarded as a structural model compound for a proposed intermediate during the hydroxylation of monophenols to catechols by tyrosinase.

Catecholase activity of copper compounds. Systematic investigations towards the catecholase activity of copper complexes have been carried out for the first time in 1980. [103] In this and several other papers it was shown that dinuclear copper complexes are in general more active than comparable mononuclear ones. [104, 105] So far, only few crystal structures of catalytically active dinuclear complexes have been described that exhibit a coordinated catechol or quinone ligand. In $[Cu_2(L\text{-}O^-)(tcc)]^+$ (where L-O$^-$ = 2,6-bis[[bis((2-pyridyl)methyl)amino]methyl] phenolate and tcc = tetrachlorocatecholate dianion) the two oxygen atoms of the tetrachlorocatecholate ligand are coordinated to different copper ions leading to a square-pyramidal coordination sphere at each metal center. [106] In 2002 a different coordination mode for the catecholate in copper complexes utilizing dinucleating pyrazol-based ligands was reported. [107] The catecholate is bound bidentately to only one copper ion in these model complexes.

Acknowledgements

The competent assistance by Dr. Adrienne Hammerschmidt in the preparation of this manuscript is gratefully acknowledged. I thank Dr. Annette Rompel, Dr. Carsten Gerdemann, and Dr. Andreas Vogel for valuable discussions.

References

[1] Fraústo da Silva, J. J. R., Williams, R. J. P., *The Biological Chemistry of the Elements*, 2nd ed., Oxford University Press, New York 2001.

[2] Bertini, I., Gray, H. B., Lippard, S. J., Valentine, J. S., *Bioinorganic Chemistry*, University Science Books, Mill Valley, CA, 1994.

[3] Kaim, W., Schwederski, B., *Bioinorganic Chemistry: Inorganic Elements in the Chemistry of Life*, John Wiley & Sons, New York, 1994.

[4] Lippard, S. J., Berg, J. M., *Principles of Bioinorganic Chemistry*, University Science Books, Mill Valley, CA, 1994.

[5] Issues of *Chemical Reviews*, e.g. 8/1994 and 11/1996.

[6] Holm, R. H., Kennepohl, P., Solomon, E. I., *Chem. Rev.* 96, 2239, 1996.

[7] Klabunde, T., Krebs, B., The Dimetal Center in Purple Acid Phosphatases, in: *Structure and Bonding* 89, 177, 1997.

[8] Dietrich, M., Münstermann, D., Suerbaum, H., Witzel, H., *Eur. J. Biochem.* 199, 105, 1991.

[9] Beck, J. L., McConachie, L. A., Summors, A. C., Arnold, W. N., De Jersey, J., Zerner, B., *Biochim. Biophys. Acta* 869, 61, 1986..

[10] Durmus, A., Eicken, C., Sift, B. H., Kratel, A., Kappl, R., Hüttermann, J., Krebs, B., *Eur. J. Biochem.* 260, 709, 1999.

[11] Schenk, G., Ge, Y., Carrington, L. E., Wynne, C. J., Searle, I. R., Carroll, B. J., Hamilton, S., De Jersey, J., *Arch. Biochem. Biophys.* 370, 183, 1999.

[12] Averill, B. A., Davis, J. C., Burman, S., Zirino, T., Sanders-Loehr, J., Loehr, T. M., Sage, J. T., Debrunner, P. G., *J. Am. Chem. Soc.* 109, 3760, 1987.

[13] Pyrz, J. W., Sage, J. T., Debrunner, P. G., Que Jr., L., *J. Biol. Chem.* 261, 11015, 1986.

[14] Crans, D. C., Simone, C. M., Holz R. C., Que Jr. L., *Biochemistry* 31, 11731, 1992.

[15] Crowder, M. W., Vincent, J. B., Averill, B. A., *Biochemistry* 31, 9603, 1992.

[16] Doi, K., Gupta, R., Aisen, P., *J. Biol. Chem.* 262, 6982, 1987

[17] Merkx, M., Averill, B. A., *Biochemistry* 37, 11223, 1998.

[18] Wang, Z., Ming, L.-J., Que Jr., L., Vincent, J. B., Crowder, M. W., Averill, B. A., *Biochemistry* 31, 5263, 1992.

[19] Holz, R. C., Que Jr., L., Ming, L.-J., *J. Am. Chem. Soc.* 114, 4434, 1992.

[20] Kauzlarich, S. M., Teo, B. K., Zirino, T., Burman, S., Davis, J. C., Averill, B. A., *Inorg. Chem.* 25, 2781, 1986.

[21] True, A. E., Scarrow, R. C., Randall, C. R., Holz, R. C., Que Jr., L., *J. Am. Chem. Soc.* 115, 4246, 1993.

[22] Priggemeyer, S., Eggers-Borkenstein, P., Ahlers, F., Henkel, G., Körner, M., Witzel, H., Nolting, H.-F., Hermes, C., Krebs, B., *Inorg Chem,* 34, 1445, 1995.

[23] Gehring, S., Fleischhauer, P., Haase, W., Dietrich, M., Witzel, H., *Biol. Chem. Hoppe-Seyler* 371, 786, 1990.

[24] Sinn, E. O., Connor, C. J., *Inorg. Chim. Acta* 78, L13, 1983.

[25] Gehring, S., Fleischhauer, P., Behlendorf, M., Hüber, M., Lorösch, J., Haase, W., Dietrich, M., Witzel, H., Löcke, R., Krebs, B., *Inorg. Chim. Acta.* 252, 13, 1996.

[26] Wang, Z., Holz, R. C., David, S. S., Que Jr., L., Stankovich, M. T., *Biochemistry* 30, 8187, 1991.

[27] Antanaitis, B. C., Strekas, T., Aisen, P., *J. Biol. Chem.* 257, 3766, 1982.

[28] Allen, M. P., Yamada, A. H., Carpenter, F. H., *Biochemistry* 22, 3778, 1983.

[29] Sträter, N., Fröhlich, R., Schiemann, A., Krebs, B., Körner, M., Suerbaum, H., Witzel, H., *J. Mol. Biol.* 224, 511, 1992.

[30] Sträter, N., Klabunde, T., Tucker, P., Witzel, H., Krebs, B., *Science* 268, 1489, 1995.

[31] Klabunde, T., Sträter, N., Fröhlich, R., Witzel, H., Krebs, B., *J. Mol. Biol.* 259, 737, 1996.

[32] Goldberg, J., Huang, H. B., Kwon, Y. G., Greengard, P., Nairn, A. C., Kuriyan, J., *Nature* 376, 745, 1995.

[33] Kissinger, C. R., Parge, H. E., Knighton, D. R., Lewis, C. T.; Pelletier, L. A., Tempczyk, A., Kalish, V. J., Tucker, K. D.; Showalter, R. E., Moomaw, E. W., Gastinel, L. N., Habuka, N., Chen, X. H., Maldonado, F., Barker, J. E., Bacquet, R., Villafranca, J. E., *Nature* 378, 641, 1995.

[34] Griffith, J. P., Kim, J. L., Kim, E. E., Sintchak, M. D., Thomson, J. A., Fitzgibbon, M. J., Fleming, M. A., Caron, P. R., Hsiao, K., Navia, M. A., *Cell*, 82, 507, 1995.

[35] Knöfel, T., Sträter, N., *Nature Struct. Biol.* 6, 448, 1999.

[36] Aquino, M. A. S., Lim, J.-S., Sykes, A. G., *J. Chem. Soc. Dalton Trans.* 429, 1994.

[37] Lindqvist, Y., Johansson, E., Kaija, H., Vihko, P., Schneider, G., *J. Mol. Biol.* 291, 135, 1999

[38] Guddat, L. W., McAlpine, A. S., Hume, D., de Jersey, J., Hamilton, S., Martin, J. L., *Acta Crystallogr. D Biol. Crystallogr.* 55, 1462, 1999.

[39] Uppenberg, J., Lindqvist, F., Svensson, C., Ek-Rylander, B., Andersson, G., *J. Mol. Biol.* 290, 201, 1999.

[40] Klabunde, T., Sträter, N., Krebs, B., Witzel, H., *FEBS Lett.* 367, 56, 1995.

[41] Ljusberg, J., Ek-Rylander, B., Andersson, G., *Biochem. J.* 343, 63, 1999.

[42] Merkx, M., Pinkse, M. W., Averill, B. A., *Biochemistry* 38, 9914, 1999.

[43] Merkx, M., Averill, B. A., *J. Am. Chem. Soc.* 121, 6683, 1999.

[44] Wang, X., Ho, R. Y. N., Whiting, A. K., Que Jr., L.,. *J. Am. Chem. Soc.* 121, 9235, 1999.

[45] Grote, M., Schwerdtfeger, C., Wiermann, R., Reichelt, R., Witzel, H., *Ann. Bot. 82*, 235, 1998.

[46] Del Pozo, J. C., Allona, I., Rubio, V., Leyva, A., De La Pena, A., Aragoncillo, C., Paz-Ares, J., *Plant J. 19*, 579, 1999.

[47] Hayman, A. R., Jones, S. J., Boyde, A., Foster, D., Colledge, W. H., Carlton, M. B., Evans, M. J., Cox, T. M., *Development* 122, 3151, 1996.

[48] Nordahl, J., Andersson, G., Reinholt, F. P., *Calcif. Tissue Int.* 63, 401, 1998.

[49] Heinegard, D., Andersson, G., Reinholt, F. P., *Ann. N Y Acad. Sci.* 760, 213, 1995.

[50] Reinholt, F. P., Hultenby, K., Heinegard, D., Marks, Jr., S. C., Norgard, M., Andersson, G., *Exp. Cell Res.* 251, 477, 1999.

[51] Schindelmeiser, J., Münstermann, D., Witzel, H., *Histochemistry* 87, 13, 1987.

[52] Hayman, A. R., Bune, A. J., Bradley, J. R., Rashbass, J., Cox, T. M., *J. Histochem. Cytochem.* 48, 219, 2000.

[53] Sträter, N., Jasper, B., Scholte, M., Krebs, B., Duff, A. P., Langley, D. B., Han, R., Averill, B. A., Freeman, H. C., Guss, J.M., *J. Mol. Biol.* 351, 233, 2005.

[54] Waratrujiwong, T., Krebs, B., Spener, F., Visoottiviseth, P., *FEBS Journal* 273, 1649, 2006.

[55] Vogel, A., Börchers, T., Marcus, K., Meyer, H. E., Krebs, B., Spener, F., *Archives Biochem. Biophy.* 401, 164, 2002,

[56] Truong, N. T., Naseri, J. I., Vogel, A., Rompel, A., Krebs, B., *Archives Biochem. Biophys.* 440, 38, 2005.

[57] Naseri, J. I., Truong, N. T., Hörentrup, J., Kuballa, P., Vogel, A., Rompel, A., Spener, F., Krebs, B., *Archives Biochem. Biophys.* 432, 25, 2004).

[58] Belle, C., Gautier-Luneau, I., Karmazin, L., Pierre, J.-L., Albedyhl, S., Krebs, B., Bonin, M., *Eur. J. Inorg Chem.* 3087, 2002.

[59] Albedyhl, S., Schnieders, D., Jancso, A., Gadja, T., Krebs, B., *Eur. J. Inorg. Chem.* 6, 1400, 2002.

[60] Albedyhl, S., Averbuch-Pouchet, M. T., Belle, C., Krebs, B., Pierre, J.-L., Saint-Aman, E., Torelli, S., *Eur. J. Inorg. Chem.* 6, 1457, 2001.

[61] Rompel, A., Gerdemann, C., Vogel, A., Krebs, B., in: *Inorganic Chemistry Highlights*, Wiley VCH, Weinheim 2002, pp. 155 ff.

[62] Kitajima, N., Fujisawa, K., Moro-oka, Y., *J. Am. Chem. Soc.* 111, 8975, 1989.

[63] Eicken, C., Zippel, F., Büldt-Karentzopoulos, K., Krebs, B., *FEBS Lett.* 436, 293, 1998.

[64] Gaykema, W. P., Volbeda, A., Hol, W. G., *J. Mol. Biol.* 187, 255, 1986.

[65] Hazes, B., Magnus, K. A., Bonaventura, C., Bonaventura, J., Dauter, Z., Kalk, K. H., Hol, W. G., *Protein Sci.* 2, 597, 1993.

[66] Cuff, M. E., Miller, K. I., van Holde, K. E., Hendrickson, W. A., *J. Mol. Biol.* 278, 855, 1998.

[67] Klabunde, T., Eicken, C., Sacchettini, J. C., Krebs, B., *Nat. Struct. Biol.* 5, 1084, 1998.

[68] Lerch, K., *J. Biol. Chem.* 257, 6414, 1982.

[69] Gielens, C., De Geest, N., Xin, X. Q., Devreese, B., Van Beeumen, J., Preaux, G., *Eur. J. Biochem.* 248, 879, 1997.

[70] Ito, N., Phillips, S. E. V., Stevens, C., Ogel, Z. B., McPherson, M. J.; Keen, J. N., Yadav, K. D. S., Knowles, P. F., *Nature* 350, 87, 1991.

[71] Rompel, A., Fischer, H., Meiwes, D., Büldt-Karentzopoulos, K., Dillinger, R., Tuczek, F., Witzel, H., Krebs, B., *J. Biol. Inorg. Chem.* 4, 56, 1999.

[72] Eicken, C., Krebs, B., Sacchettini, J. C., *Curr. Opin. Struc. Biol.* 9, 677,1999.

[73] Volbeda, A., Hol, W. G. J., *J. Mol. Biol.* 209, 249, 1989.

[74] Salvato, B., Santamaria, M., Beltramini, M., Alzuet, G., Casella, L., *Biochemistry* 37, 14065, 1998.

[75] Solomon, E. I., Lowery, M. D., *Science* 259, 1575, 1993.

[76] Solomon, E. I., Sundaram, U. M., Machonkin, T. E., *Chem. Rev.* 96, 2563, 1996.
[77] Moro-oka, Y., Fujisawa, K., Kitajima, N., *Pure Appl. Chem.* 67, 241, 1995.
[78] Holland, P. L., Tolman, W. B., *Coord. Chem. Rev.* 192, 855, 1999.
[79] Itoh, S., Taki, M., Nakao, H., Holland, P. L., Tolman, W. B., Que Jr., L., Fukuzumi, S., *Angew. Chem. Int. Ed.* 39, 398, 2000.
[80] Walker, J. R., Ferrar, P. H., *Biotechnol. Genet. Eng. Rev.* 15, 457, 1998.
[81] Boss, P. K., Gaudner, R. C., Janssen, B.-J., Ross, G. S., *Plant Mol. Biol.* 27, 429, 1995.
[82] Vaugh, K. C., Lax, A. R., Duke, S. O., *Physiol. Plant* 72, 659, 1988.
[83] Ueda, T., Nakao, M., Tanaka, Y., Kusumi, T., Nishino, T., *Science* 290, 1163, 2000.
[84] Karlin, K.D.; Kaderli, S.; Zuberbühler, A.D. *Acc. Chem. Res.* 30, 139, 1997.
[85] Fox, S.; Karlin, K. D. *Active Oxygen in Biochemistry* (Eds. J. S. Valentine, C. S. Foote, A. Greenberg, J. F. Liebman), Chapman & Hall: Glasgow, Scotland 1995, pp. 188 ff.
[86] Kitajima, N.; Tolman, W.B. *Prog. Inorg. Chem.* 43, 419, 1995.
[87] Tolman, W.B. *Acc. Chem. Res.* 30, 227, 1997.
[88] Solomon, E.I.; Tuczek, F.; Root, D.E.; Brown, C.A. *Chem. Rev.* 94, 827, 1994.
[89] Kitajima, N.; Moro-oka, Y. *Chem. Rev.* 94, 737, 1994
[90] Karlin, K.D.; Tyeklár, Z. *Adv. Inorg. Biochem.* 9, 123, 1994.
[91] Kitajima, N.; Moro-oka, Y. *J. Chem. Soc., Dalton Trans.* 2665, 1993.
[92] Sorrell, T.N. *Tetrahedron* 45, 3, 1989.
[93] Tyeklár, Z.; Karlin, K.D. *Acc. Chem. Res.* 22, 241, 1989.
[94] Krebs, B., Merkel, M., Rompel, A., Catechol oxidase and biomimetic approaches, *J. Argent. Chem. Soc.* 92, 1, 2004.
[95] Karlin, K.D.; Tyeklár, Z.; Farooq, A.; Jacobson, R.R.; Sinn, E.; Lee, D.W.J.; Bradshaw, E.; Wilson, L.J. *Inorg. Chim. Acta* 182, 1, 1991.
[96] Kitajima, N.; Fujisawa, K.; Fujimoto, C.; Moro-oka, Y.; Hashimoto, S.; Kitagawa, T. Toriumi, K.; Tatsumi, K.; Nakamura, A. *J. Am. Chem. Soc.* 114, 1277, 1992.
[97] Hu, Z.; George, G.N.; Gorun, S.M. *Inorg. Chem.* 40, 4812, 2001.
[98] Kodera, M.; Katayama, K.; Tachi, Y.; Kano, K.; Hirota, S.; Fujinami, S.; Suzuki, M. *J. Am. Chem. Soc.* 121, 11006, 1999.
[99] Santagostini, L.; Gullotti, M.; Monzani, E.; Casella, L.; Dillinger, R.; Tuczek, F. *Chem. Eur. J.* 6, 519, 2000.
[100] Gentschev, P.; Lüken, M.; Möller, N.; Rompel, A.; Krebs, B. *Inorg. Chem. Commun.* 4, 753, 2001.
[101] Neves, A.; Rossi, L.M.; Horn Jr., A.; Vencato, I.; Bortoluzzi, A.J.; Zucco, C.; A. S. Mangrich, *Inorg. Chem. Comm.* 2, 334, 1999.
[102] Neves, A.; Rossi, L.M.; Vencato, I.; Drago, V.; Haase, W.; Werner, R. *Inorg. Chim. Acta* 281, 111, 1998.
[103] Oishi, N.; Nishida, Y.; Ida, K.; Kida, S. *Bull. Chem. Soc. Jpn.*, 53, 2847, 1980.
[104] Casellato, U.; Tamburini, S.; Vigato, P.A.; de Stefani, A.; Vidali, M.; Fenton, D.E. *Inorg. Chim. Acta* 69, 45, 1983.
[105] Malachowski, M.R.; Davidson, M.G. *Inorg. Chim. Acta* 162, 199, 1989.
[106] Karlin, K.D.; Gultneh, Y.; Nicholson, T.; Zubieta, J. *Inorg. Chem.* 24, 3727, 1985.
[107] Ackermann, J.; Meyer, F.; Kiefer, E.; Pritzkow, H. *Chem. Eur. J.* 8, 247, 2002.

Manuscrito recibido el 24 de setiembre de 2007.
Aceptado el 11 de octubre de 2007.